

# Kinetic characterization of active site mutants Ser402Ala and Phe397His of vanadium chloroperoxidase from the fungus *Curvularia inaequalis*

Naoko Tanaka, Zulfiqar Hasan, Ron Wever\*

*Institute for Molecular Chemistry, University of Amsterdam, Nieuwe Achtergracht 129, 1018 WS Amsterdam, The Netherlands*

Received 1 April 2003; accepted 16 July 2003

Dedicated to Professor J. Fraústo da Silva on the occasion of his retirement

## Abstract

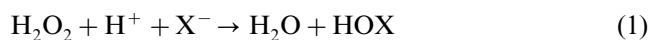
Site-directed mutagenesis was performed on two conserved active site residues of vanadium chloroperoxidase (VCPO) from the fungus *Curvularia inaequalis*. Mutation of an active site residue Ser402 to Ala (S402A), a residue proposed to be brominated during turnover, caused a decrease in its activity, however it still catalyses efficiently the oxidation of both chloride and bromide. The  $K_m$  values for chloride and bromide of S402A at the optimal pH 4.5 were 3.2 mM and 20  $\mu$ M, respectively. The active site residues of VCPO and vanadium bromoperoxidases (VBPO) from the seaweeds *Ascophyllum nodosum* and *Corallina officinalis* show very high similarity. A prominent difference in the active site architecture of VCPO and VBPO is the presence of a second histidine in VBPO, a residue substituted by a phenylalanine in VCPO. The mutation of Phe397 to His (F397H) resulted in the enhancement of bromination activity under certain conditions. However, inactivation of F397H by halide especially at low pH was observed during turnover. Kinetic parameters and characteristics of these mutants are discussed in this report. A detailed kinetic analysis of the pH dependence of the chlorinating and brominating activity of VCPO and the S402A yielded an interesting difference between the two activities. The results show that the  $K_m$  for  $\text{Cl}^-$  was pH dependent whereas the  $K_m$  for  $\text{Br}^-$  was hardly pH dependent. The data confirm that protonation of an active site residue or the bound peroxide is essential for chloride oxidation.

© 2003 Elsevier B.V. All rights reserved.

**Keywords:** Vanadium chloroperoxidase; Vanadium bromoperoxidase; Active site mutants; Chlorinating activity

## 1. Introduction

Vanadium haloperoxidases are enzymes that catalyse the oxidation of a halide ( $\text{X}^-$ ) by hydrogen peroxide to the corresponding hypohalous acids according to Eq. (1).



**Abbreviations:** rVCPO, recombinant wild type vanadium chloroperoxidase (SWISS-PROT primary accession number P49053); VBPO, vanadium bromoperoxidase; S402A, vanadium chloroperoxidase mutant Ser402 to Ala; F397H, vanadium chloroperoxidase mutant Phe397 to His.

\* Corresponding author. Tel.: +31-20-525-5110; fax: +31-20-525-5670.

E-mail address: [rwever@science.uva.nl](mailto:rwever@science.uva.nl) (R. Wever).

The enzymes are named after the most electronegative halide ion they are able to oxidize, therefore chloroperoxidase (CPO) oxidizes  $\text{Cl}^-$ ,  $\text{Br}^-$ ,  $\text{I}^-$  and bromoperoxidase (BPO) oxidizes  $\text{Br}^-$  and  $\text{I}^-$ . This class of enzymes binds vanadate ( $\text{HVO}_4^{2-}$ ) as a prosthetic group [1,2]. The crystal structures [3–6] of vanadium chloroperoxidase (VCPO) from the fungus *Curvularia inaequalis* and bromoperoxidase (VBPO) from the brown seaweed *Ascophyllum nodosum* and the red algae *Corallina officinalis* show that vanadate in these enzymes is covalently attached to a histidine (i.e.  $\text{N}^{\epsilon 2}$  of His496 in VCPO) while five residues (i.e. Arg360, Arg490, Lys353, Ser402 and Gly403 in VCPO) donate hydrogen bonds to the non-protein oxygens. The resulting structure is that of a trigonal bipyramid with three non-protein oxygens in the equatorial plane (Fig. 1(A)). The fourth oxygen (hydroxide group) and the

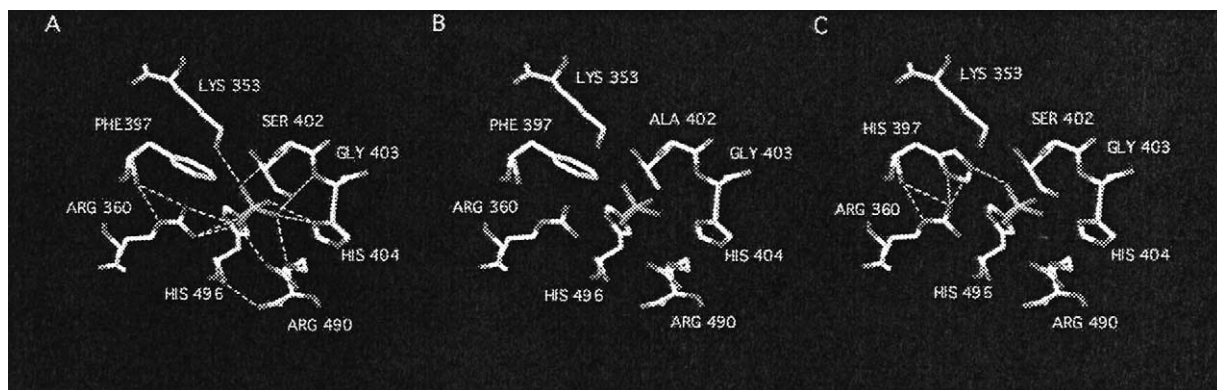


Fig. 1. Active site structure comparison of (A) vanadium chloroperoxidase from *C. inaequalis* (Protein Data Bank entry: 1IDQ), (B) VCPO mutant S402A and (C) F397H. Dotted lines indicate hydrogen bonds. In panel C, expected extra hydrogen bonds by the mutation are shown. The figure was prepared and modelled using Swiss PDB Viewer.

nitrogen atom from a histidine residue are at the apical positions. Steady-state kinetics of both VCPO and VBPO support a model in which a vanadium peroxo intermediate is formed during catalysis prior to oxidation of the halide. Indeed the crystal structure of the peroxide intermediate has been obtained in which the peroxide is bound side-on [4]. Hemrika et al. studied the cofactor binding residues of VCPO by site-directed mutagenesis [7], showing the importance of the binding residue His496 and positively charged residues. They proposed that the positively charged residues Arg360 and Arg490 enhance the withdrawal of electron density from the bound peroxide and that Lys353 polarises the bound peroxide. The above mentioned vanadate-binding amino acids were shown to be conserved in two bromoperoxidases from seaweed and several acid phosphatases among others the large group of soluble bacterial non-specific class A acid phosphatases [3,8–13]. Based on sequence similarity it has been proposed [8–12] that the architecture of the active site in the two classes of enzymes is very similar. More recently this was confirmed by the X-ray structure of the acid phosphatase from *Escherichia blattae* [13]. It has been shown that apo CPO [8] and apo BPO [14] have phosphatase activity and vanadate substituted acid phosphatases have bromoperoxidase activity [15].

Based on bromine K-edge EXAFS studies of VBPO [16], Dau et al. proposed that the serine residue in the active site is the site of bromination and may play a role in catalysis. We demonstrated here that mutation of Ser402 of VCPO to alanine (S402A, Fig. 1(B)) has a relatively minor effect on the catalytic activity.

According to the crystal structure of VCPO from *C. inaequalis* [3,4] and VBPO from *A. nodosum* and *C. officinalis* [5,6], VBPOs contain a histidine residue (i.e. His411 of *A. nodosum* VBPO and His478 [6] or His480 [17] of *C. officinalis* VBPO, respectively) instead of Phe397 in VCPO. It has been proposed [5,7,18] that the histidine residue in VBPO may play a role in protona-

tion or deprotonation of the peroxide intermediate in the active site because His411 of *A. nodosum* VCPO is within hydrogen bonding distance of a modelled peroxo vanadate. The mutation of Phe397 in rVCPO to a His as modelled in Fig. 1(C) may result in additional hydrogen bonds. In recombinant VBPO from *C. officinalis* the effect of mutating the histidine residue into alanine has been examined [17], showing the loss of the ability to oxidise bromide. However, the enzyme was still able to oxidise iodide. Similarly mutation of the residue Arg490, Arg360 and Lys353 into Ala in VCPO resulted in loss of chlorinating activity, but the enzyme was still able to oxidise bromide [7,18]. In this report we studied the effect of mutation of Phe397 into His (F397H). We show that this results in partial loss of chloroperoxidase activity, but surprisingly in the bromination reaction the mutant showed a higher  $k_{\text{cat}}$  at high pH values than the recombinant wild type enzyme.

## 2. Experimental

### 2.1. Materials

All restriction enzymes were purchased from Roche Diagnostics (Nederland B.V). QuikChange™ Site-directed Mutagenesis Kit was obtained from Stratagene (La Jolla, CA). *Escherichia coli* strains TOP 10 (Invitrogen) was used for propagation of recombinant DNA constructs. *Saccharomyces cerevisiae* strain BJ1991 (*Mat $\alpha$* , *leu2*, *trp2*, *ura3-251*, *prb1-1122*, *pep4-3*) was used as the expression host.

### 2.2. Site-directed mutagenesis and protein expression

The site-directed mutants were created in the expression vector pTNT14 [7] by Quikchange™ site-directed mutagenesis kit according to the protocol provided by the suppliers. The oligonucleotides used to direct the

mutation Phe397 to His were F397H 5'-CCATT-CAAGCTCCTCACCCAGCTTACCCATCTG-3' and its complementary primer F397H(C) 5'-CA-GATGGGTAAGCTGGGTGAGGAGGCTTGAAT-GG-3'. Primers used to direct mutation Ser402 into Ala were S402A 5'-CCAGCTTACCCAGCTGGTCACGC-GACC-3' and S402A(C) 5'-GGTCGCGTGAC-CAGCTGGGTAAGCTGG-3'. The mismatched nucleotide(s) have been underlined. The changes were confirmed on both strands by automated sequencing (MWG Biotech, Germany). In addition, the S402A mutation was also confirmed by restriction digestion as the mutation resulted in the creation of a Pvu II restriction site. The pTNT14 derivatives were transformed to *S. cerevisiae* BJ1991 for protein expression. Enzyme variants were expressed and purified essentially as described by Hemrika et al. [7].

The purity of the preparations was checked on SDS-PAGE gels stained with Coomassie brilliant blue R-250, and the protein concentration was determined by using a protein assay kit (Bio-Rad) with BSA as the standard.

### 2.3. Enzyme activity assays

During purification VCPO activity can be qualitatively tested using the phenol red assay by incubating the enzyme in 100 mM sodium citrate (pH 5), 40  $\mu$ M phenol red, 100  $\mu$ M orthovanadate, 10–100 mM KBr and 10 mM H<sub>2</sub>O<sub>2</sub>. Active fractions show a large colour changes from red to blue [19].

Quantitative VCPO activity was measured by monitoring the chlorination or bromination of monochlorodimedone (MCD,  $\epsilon = 20.2 \text{ mM}^{-1} \text{ cm}^{-1}$  at 290 nm) to dichlorodimedon or monobromo–monochlorodimedon ( $\epsilon = 0.1 \text{ mM}^{-1} \text{ cm}^{-1}$  at 290 nm) in 100 mM sodium citrate (pH range of 3.5–6.3) and using the appropriate concentrations of the substrates; chloride or bromide and H<sub>2</sub>O<sub>2</sub> [8]. Since the recombinant CPO is produced as apo-enzyme by the yeast expression system [7,8], recombinant mutants (10  $\mu$ M) were preincubated with 100  $\mu$ M orthovanadate in 100 mM Tris–acetate (pH 8.3) prior to the activity assay. The kinetic parameters were determined by non-linear regression using the EnzymeKinetics program (Trinity Software). In this report, the data points are means of at least triplicate measurements, unless otherwise mentioned.

## 3. Results

### 3.1. Expression and purification of recombinant VCPO S402A and F397H

Recombinant CPO (rCPO) S402A and F397H were overexpressed as apo-enzyme in *S. cerevisiae* with over 95% purity. On average, the yield of these mutants was

approximately 10 and 80 mg (S402A and F3967H, respectively) per litre of culture.

### 3.2. Comparison of rVCPO and mutant S402A and F397H at different pH

Since VCPO mutants S402A and F397H were isolated as apo-enzymes, they were reconstituted by preincubation with 100  $\mu$ M orthovanadate in 100 mM Tris–acetate (pH 8.3). The chlorination activity was measured by MCD assay containing 5 mM NaCl, 1 mM H<sub>2</sub>O<sub>2</sub>, 50  $\mu$ M MCD at pH 5.0. Both mutants were fully activated by 100  $\mu$ M orthovanadate in 100 mM Tris–acetate (pH 8.3) within 5 min and showed chlorination activity (results not shown). The quick reconstitution of vanadate, a typical property of VCPO, was not affected by the introduced mutations.

The chlorinating activities of S402A and F397H and that of rVCPO at several substrate conditions are illustrated in Fig. 2. Under the standard assay condition for rVCPO (5mM NaCl and 1 mM H<sub>2</sub>O<sub>2</sub> at pH 3.5–6.0), F397H had a specific activity of 2.6 U mg<sup>-1</sup> at pH 4.5 which is approximately 12% of that of rVCPO (22 U mg<sup>-1</sup>). S402A had only 1.8% activity (0.46 U mg<sup>-1</sup>) compared to rVCPO. Both rVCPO as well as the S402A showed an optimum at pH 4.5 in line with van Schijndel et al. [2]. It was not possible to obtain data for F397H at low pH since inactivation was observed during turnover. Despite the decrease in chlorination activity it is obvious that these mutations did not affect dramatically the halogenation activity of the enzyme. Most of the mutations reported previously [7,18] resulted into the loss of chlorination ability and large increases in  $K_m$  values for both chloride and H<sub>2</sub>O<sub>2</sub>. Fig. 2(B–D) show the bromination activity of enzyme mutants at 10 mM H<sub>2</sub>O<sub>2</sub>, and it is clear by comparison of Panel C and D, 1 and 5 mM KBr, respectively, that rVCPO is inhibited by high concentration of bromide.

Similarly, mutant S402A showed inhibition by bromide, although it is less pronounced. Surprisingly F397H showed an increase in activity at higher bromide as is illustrated in Fig. 2(D). This result suggests that F397H is a better bromoperoxidase than rVCPO at high bromide concentration.

### 3.3. Kinetic properties of mutant S402A

To determine the detailed kinetic properties of mutant S402A, the enzymatic activities using several concentrations of Br<sup>-</sup>, Cl<sup>-</sup> and H<sub>2</sub>O<sub>2</sub> as substrates were measured as a function of pH. Fig. 3 shows the kinetic parameters  $k_{\text{cat}}$ ,  $\log K_m$  and  $k_{\text{cat}}/K_m$  of mutant S402A when Br<sup>-</sup> was used as substrate at a fixed concentration of H<sub>2</sub>O<sub>2</sub> (2mM). The optimum pH for S402A as well as rVCPO was around pH 4.5. Although  $k_{\text{cat}}$  of rVCPO decreased from 300 to 92 s<sup>-1</sup> for the S402A mutant at

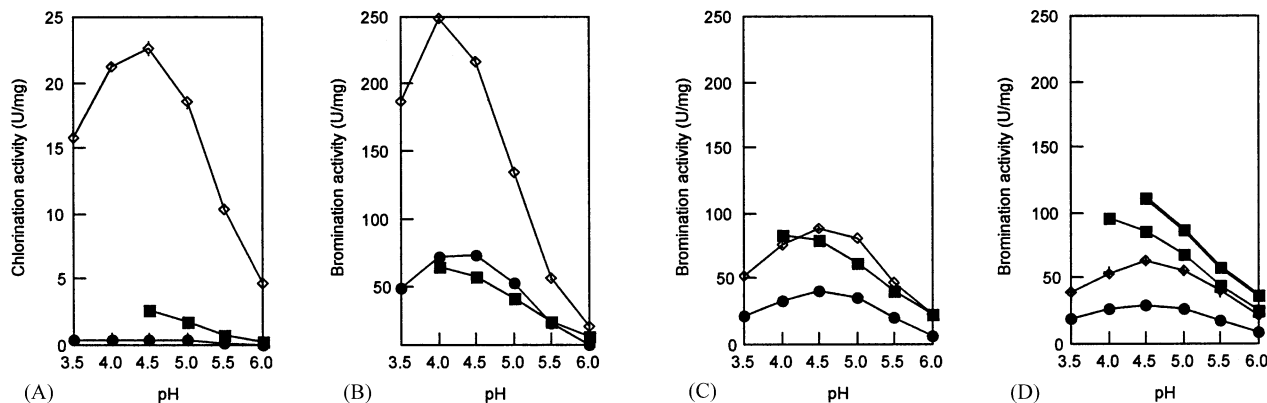


Fig. 2. Halogenation activity of rVCPO ( $\diamond$ ), mutant S402A ( $\bullet$ ) and F397H ( $\blacksquare$ ) as a function of pH. (A) 5 mM NaCl and 1 mM  $\text{H}_2\text{O}_2$ . (B) 0.1 mM KBr and 10 mM  $\text{H}_2\text{O}_2$ . (C) 1 mM KBr and 10 mM  $\text{H}_2\text{O}_2$  and (D) 5 mM or 10 mM (thick line) KBr and 10 mM  $\text{H}_2\text{O}_2$ . The data points are means of duplicate measurements.

pH 4.5 (Fig. 3(A)), the  $K_m$  for  $\text{Br}^-$  was not strongly affected by the mutation (Fig. 3(B)). The pH dependence of the  $K_m$  for bromide was also determined and it is clear that the  $K_m$  for VCPO and the mutant are hardly pH dependent. The inset in Fig. 3(B) shows that the  $K_m$  for  $\text{Br}^-$  changes from 11 to 20  $\mu\text{M}$  and from 7 to 19  $\mu\text{M}$  for S402A and rVCPO, respectively in the pH range of 3.5–6.3. As seen with VCPO [20,21] and Fig. 2(B–D) of this report, the inhibition of S402A by bromide is observed especially at low pH. Between pH 3.5 and 4.5, a concentration greater than 200  $\mu\text{M}$   $\text{Br}^-$  inhibited the S402A, between pH 5.0 and 5.5 only concentrations greater than 500  $\mu\text{M}$   $\text{Br}^-$  had an effect, and between pH 6.0 and 6.3 500  $\mu\text{M}$   $\text{Br}^-$  did not inhibit the mutant (results not shown). The specificity constant  $k_{\text{cat}}/K_m$  value for S402A was approximately one sixth of that for rVCPO (Fig. 3(C)). The pH dependence is similar to that of the  $k_{\text{cat}}$  values because the  $K_m$  values for S402A and rVCPO do not significantly differ from each other.

The  $k_{\text{cat}}/K_m$  values imply that S402A and rVCPO have similar specificity towards bromide at high pH. At low pH there is significant difference and the mutation apparently affects the binding of bromide considerably.

The kinetic parameters for  $\text{Cl}^-$  oxidation by S402A and rVCPO are shown in Fig. 4. Interestingly, the  $k_{\text{cat}}$  of S402A increases marginally at higher pH, which differs from the pH dependence of rVCPO that shows an optimum around pH 4.5–5.0 (Fig. 4(A)). As a result of this mutation, the  $k_{\text{cat}}$  of rVCPO (23  $\text{s}^{-1}$ ) decreases to 0.95  $\text{s}^{-1}$  at pH 4.5, and from 7.3 to 1.4  $\text{sec}^{-1}$  at pH 6.3. Fig. 4(B) illustrates that the  $K_m$  for chloride of both S402A and rVCPO are strongly pH dependent. The  $\log K_m$  of each enzyme species increases linearly with pH with a slope of 0.8 and 0.6 for S402A and rVCPO, respectively. The  $K_m$  of S402A increases from 1.0 to 174 mM as pH increases, whereas that of rVCPO changes from 0.23 to 10 mM. This is in a clear contrast to the pH dependence of the  $K_m$  for bromide (Fig. 3(B)). The  $K_m$

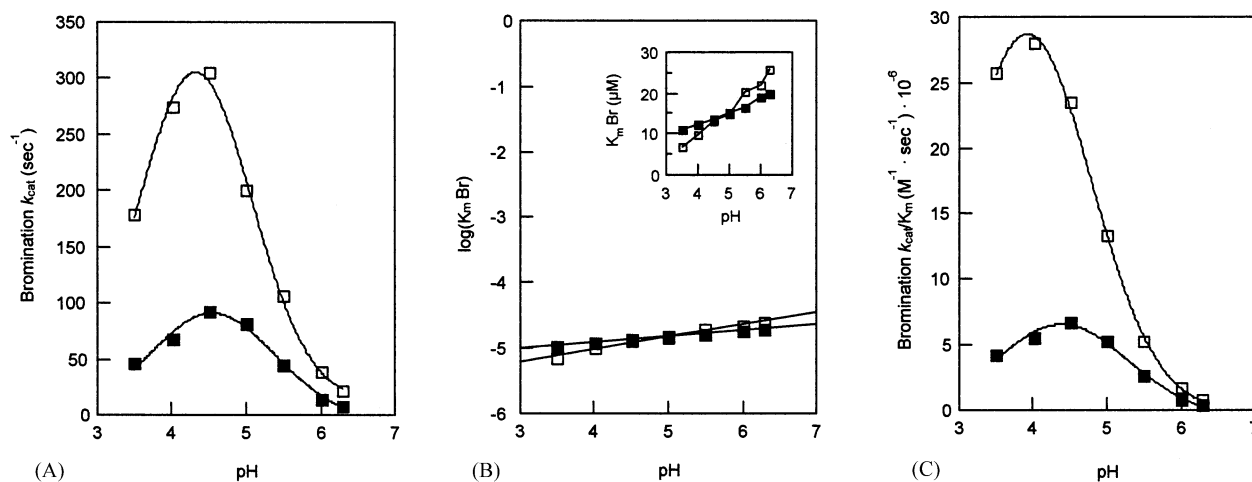


Fig. 3. Kinetic values (A)  $k_{\text{cat}}$ , (B)  $\log K_m$  and (C)  $k_{\text{cat}}/K_m$  of mutant S402A ( $\blacksquare$ ) and rVCPO ( $\square$ ) for bromide as a function of pH. Panel B inset shows the  $K_m$  for bromide. Parameters were determined by non-linear regression using EnzymeKinetics (Trinity Software). Measurements were performed at a fixed hydrogen peroxide concentration of 2 mM with at least six different KBr concentration, and 100 mM sodium citrate was used as a buffer. Final enzyme concentration was 10 nM.



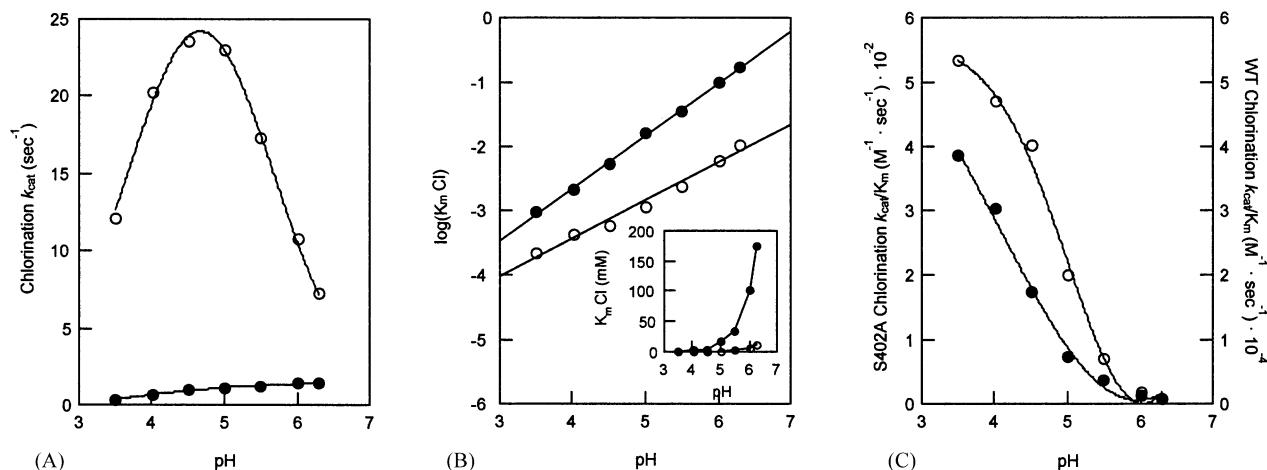


Fig. 4. Kinetic values (A)  $k_{cat}$ , (B)  $\log K_m$  and (C)  $k_{cat}/K_m$  of mutant S402A (●) and rVCPO (○) for chloride as a function of pH. Panel B inset shows the  $K_m$  for chloride. Parameters were determined by non-linear regression using EnzymeKinetics (Trinity Software). Measurements were performed at a fixed hydrogen peroxide concentration of 2 mM with at least six different NaCl concentrations, and 100 mM sodium citrate was used as a buffer. Final enzyme concentrations were 100 nM for the mutants S402A and 50 nM for rVCPO, respectively.

values for  $\text{Cl}^-$  of rVCPO and the pH dependence found here are similar to that of native VCPO from *C. inaequalis* [2]. The specificity constant  $k_{cat}/K_m$  value for S402A is approximately 100-fold lower than that of rVCPO (Fig. 4(C)), showing a significant decrease of specificity towards chloride caused by the mutation.

Fig. 5 shows the kinetic parameters for  $\text{H}_2\text{O}_2$  which were determined at a fixed concentration of 0.1 mM KBr. Since these experiments were performed with  $\text{Br}^-$ ,  $k_{cat}$  values (Fig. 5(A)) of both enzyme series are quite similar to those shown in Fig. 3(A). The  $K_m$  values for  $\text{H}_2\text{O}_2$  of S402A and rVCPO both decreased strongly as the pH increases. However, unlike for  $\text{Br}^-$ , the  $\log K_m$  for  $\text{H}_2\text{O}_2$  decreased with a slope of  $-1.0$  and  $-0.8$  for S402A and rVCPO, respectively. At low pH, the difference in  $K_m$  for S402A and rVCPO is significant

(Fig. 5(C) inset, 1.5 mM and 310  $\mu\text{M}$ , respectively), but at higher pH, the  $K_m$  values became smaller than 10  $\mu\text{M}$  and are difficult to determine exactly. The difference in the specificity constant between S402A and rVCPO becomes smaller as the pH increases (Fig. 5(C)). The specificity of S402A towards  $\text{H}_2\text{O}_2$  at high pH is nearly the same as rVCPO.

#### 3.4. Kinetic properties of mutant F397H

The steady-state rate of MCD bromination by both rVCPO and S402A are linear in time (not shown). However for F397H at pH 3.5 and 4.0, the rate of MCD bromination decreases during turnover, when the reaction was initiated by addition of enzyme. This made the initial rate measurements very difficult. A similar

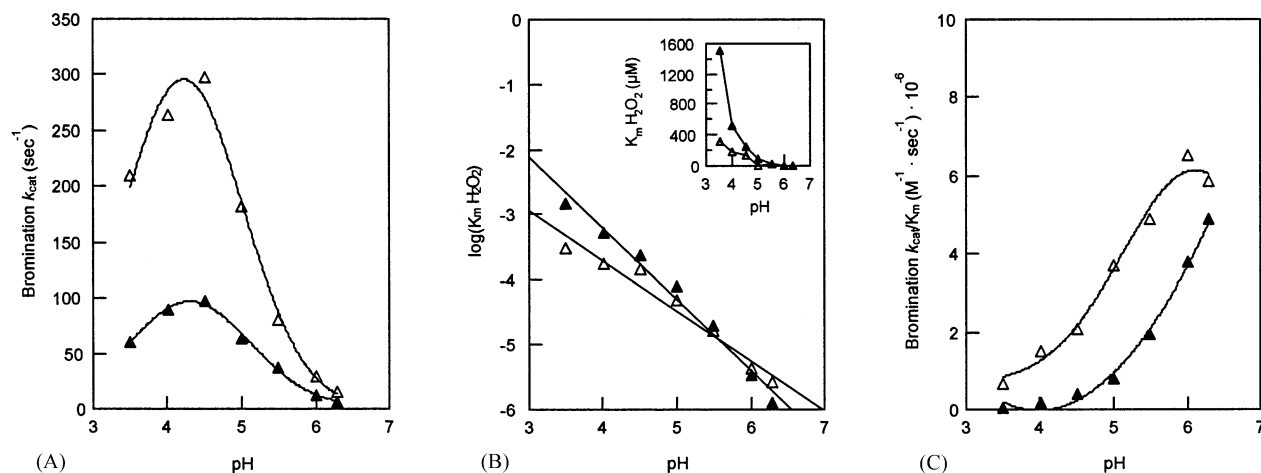


Fig. 5. Kinetic values (A)  $k_{cat}$ , (B)  $\log K_m$  and (C)  $k_{cat}/K_m$  of mutant S402A (▲) and rVCPO (△) for hydrogen peroxide as a function of pH. Panel B inset shows the  $K_m$  for hydrogen peroxide. Parameters were determined by non-linear regression using EnzymeKinetics (Trinity Software). Measurements were performed at a fixed KBr concentration of 0.1 mM with at least six different hydrogen peroxide concentrations, and 100 mM sodium citrate was used as a buffer. Final enzyme concentration was 10 nM.

inactivation in time occurred at pH 4.5 at high concentration of bromide. In addition, when the reactions were started with addition of bromide, following preincubation of enzyme with  $\text{H}_2\text{O}_2$  to form the pervanadate complex, inactivation was also observed during the time course of the MCD assay (results not shown). This suggested that bromide was responsible for the inactivation. Therefore, the MCD activity assay was carried out in different ways. The reaction was started by either addition of bromide,  $\text{H}_2\text{O}_2$  or enzyme (Fig. 6). The rate of bromination by F397H decreased significantly when F397H was preincubated with  $\text{Br}^-$ . As shown in Fig. 6(A) trace  $b_1$ – $b_5$ , longer incubation times resulted in larger inhibition of F397H. After 2 min incubation of F397H with KBr, the activity was only 20% (see also Fig. 6(C)) of F397H compared to that seen when the reaction was started by the addition of enzyme (Fig. 6(A) trace a). When KBr was added to initiate the reaction (Fig. 6(A) trace c), the rate of bromination was

nearly equal to trace a, which clearly shows that the inhibition was caused by the interaction of  $\text{Br}^-$  with of F397H and is time dependent. A similar phenomenon was found when 40  $\mu\text{M}$  KBr was used in the assay (results not shown), which implies that the affinity of the site for bromide causing the inhibition is very high. Chloride incubation also affected the enzyme activity but was not as strong as that of bromide. Fig. 6(B) shows the traces of MCD chlorination assay with 100 mM  $\text{Cl}^-$ , 10 mM  $\text{H}_2\text{O}_2$  in 100 mM sodium citrate (pH 5.0) with 100 nM F397H. The chlorination activity decreased somewhat when chloride and F397H were preincubated for 2 min (Fig. 6(B) and (C)).

Because of this inhibition by halides it was very difficult to perform a proper kinetic characterization of F397H, therefore, activities were measured only at pH 5.0 and 6.3. In addition, the inactivation was more pronounced when a low concentration of  $\text{H}_2\text{O}_2$  was used (results not shown), suggest that there may also be a

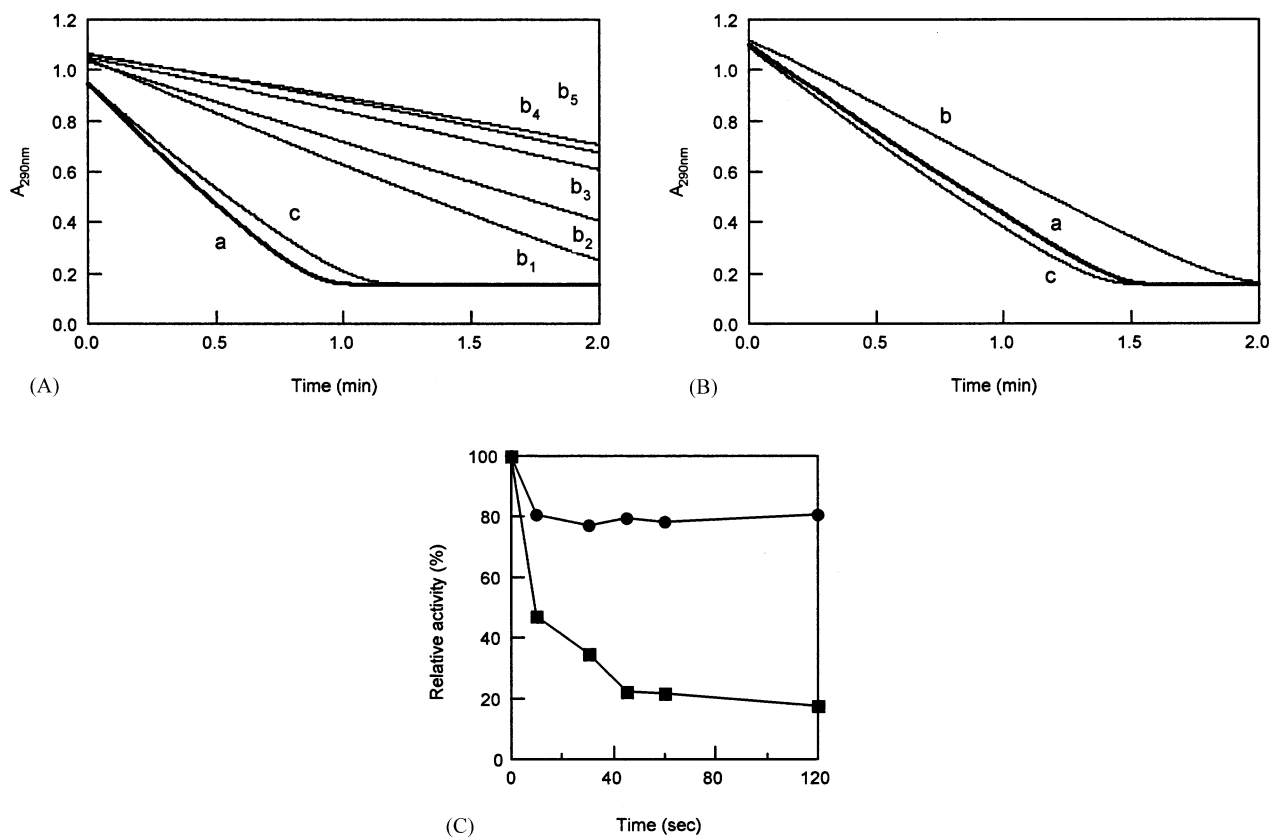


Fig. 6. Inactivation of F397H by (A) bromide and (B) chloride. Panel A, MCD assay containing 100 mM sodium citrate (pH 5.0), 50  $\mu\text{M}$  MCD, 1 mM KBr, 10 mM  $\text{H}_2\text{O}_2$  and F397H (10 nM). Trace a, the reaction was initiated by addition of enzyme. Trace  $b_1$ : F397H was incubated in the assay mixture (without  $\text{H}_2\text{O}_2$ ) for 10 s, and reaction was started by addition of  $\text{H}_2\text{O}_2$ . Trace  $b_2$ : 30 s incubation. Trace  $b_3$ : 45 s incubation. Trace  $b_4$ : 60 s incubation. Trace  $b_5$ : 120 s incubation. Trace c: F397H was incubated in the assay mixture (without KBr) for 120 s, and reaction was started by addition of 1 mM KBr. Panel B, MCD assay containing 100 mM sodium citrate (pH 5.0), 50  $\mu\text{M}$  MCD, 100 mM NaCl, 10 mM  $\text{H}_2\text{O}_2$  and F397H (100 nM). Trace a: reaction was started by addition of enzyme. Trace b: F397H was incubated in the assay mixture (without  $\text{H}_2\text{O}_2$ ) for 120 s, and reaction was started by addition of 10 mM  $\text{H}_2\text{O}_2$ . Trace c: F397H was incubated in the assay mixture (without NaCl) for 120 s, and reaction was started by addition of 100 mM NaCl. Panel C, inactivation of F397H by bromide (■) and chloride (●) as a function of time. The relative activity was obtained from trace a in panel A and B, respectively, as a standard. F397H (10  $\mu\text{M}$ ) was preincubated with 100  $\mu\text{M}$  orthovanadate in 100 mM Tris-acetate (pH 8.3) prior to the activity measurements.

competition between halide and  $\text{H}_2\text{O}_2$  in the active site. Because of the limitation in the  $\text{H}_2\text{O}_2$  concentration that could be used, we were unable to determine kinetic parameters for  $\text{H}_2\text{O}_2$ , and all measurements were performed at a fixed concentration of  $\text{H}_2\text{O}_2$  (10 mM). Table 1 summarises the kinetic parameters for rVCPO, mutant S402A and F397H.

#### 4. Discussion

##### 4.1. Haloperoxidase activity of S402A

The residue Ser402 in the active site of VCPO is one of seven residues involved in vanadate binding [3]. Moreover the EXAFS studies on the active site of VBPO from *A. nodosum* by Dau et al. [16] suggested that the active site serine residue formed a carbon-bromine bond during turnover. Site-directed mutagenesis of this residue (Ser402 to Ala) provides us an opportunity to verify the role of Ser402 in the vanadate binding and the catalytic process.

The mutation of Ser402 residue to Ala in VCPO resulted in tuning down the rate of activity of the enzyme (4.4% chlorination and 20% bromination of rVCPO at pH 4.5). However, the  $K_m$  values for substrates of S402A were comparable to that of rVCPO. The  $K_m$  values for bromide and  $\text{H}_2\text{O}_2$  were nearly the same as that of rVCPO, and the  $K_m$  value for chloride was approximately a factor of 10 higher than rVCPO at every pH value. There was striking difference in the pH dependence for bromide and chloride oxidation. The  $K_m$  value for bromide was not significantly dependent upon pH, whereas the  $K_m$  value for chloride was strongly dependent upon pH. These observations confirm earlier proposals that the chloride oxidation mechanism requires protonation of the activated vanadium peroxocomplex in the active site as proposed previously [7,18,20] (Fig. 7 illustrates this proposal). In addition, model studies suggested the necessity of the addition of

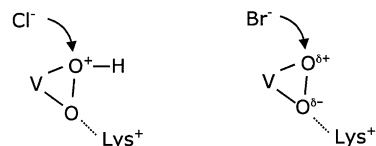


Fig. 7. Protonation state of the side-on-bound peroxide that is postulated to be attacked by the incoming halide. Left; strongly oxidizing protonated form of the side-on bound peroxide. Right; less oxidizing unprotonated form of the side-on bound peroxide.

acid for halide oxidation on each turnover [22]. The  $K_m$  value for  $\text{H}_2\text{O}_2$  is also strongly pH dependent, but in contrast to the  $K_m$  for  $\text{Cl}^-$  it increases strongly at low pH. This has been explained before by the presence of protonable groups that at low pH prevents binding of peroxide [20]. Vanadate coordinated water or a histidine residue were indicated as possible active site groups with a  $\text{p}K_a$  value in the range pH 5.6–6.5 and His404 at the active site is a likely candidate [7].

Our study clearly shows that the S402A mutant is still able to catalyse the oxidation of halides. This is contrary to the suggestions that the serine residue is involved in bromide binding during turnover [16,23]. If the Ser402 hydroxyl moiety is critical in the bromide binding step, the mutation from serine to alanine should abolish this reaction. Therefore, despite the decrease in S402A activity compared to rVCPO, the serine residue is not too crucial for the halogenation activity of this enzyme. In addition, the specificity constants for both bromine and  $\text{H}_2\text{O}_2$  upon bromination were not strongly affected compared to rVCPO especially at high pH, showing that the mutation Ser402 to Ala had a minor effect on bromination. Structural evidence from *C. officinalis* VBPO [24] indicates that the solvent accessibility of the corresponding serine (Ser483) seems to be too low in the phosphate bound form of the enzyme and support the idea that this residue has minimal role in the bromine binding.

Table 1  
Kinetic parameters of rVCPO and mutants S402A and F397H

VCPO	Substrate pH	$\text{Br}^-$			$\text{Cl}^-$			$\text{H}_2\text{O}_2$		
		$K_m$ ( $\mu\text{M}$ )	$k_{\text{cat}}$ ( $\text{s}^{-1}$ )	$k_{\text{cat}}/K_m$ ( $\text{M}^{-1} \text{s}^{-1}$ )	$K_m$ ( $\mu\text{M}$ )	$k_{\text{cat}}$ ( $\text{s}^{-1}$ )	$k_{\text{cat}}/K_m$ ( $\text{M}^{-1} \text{s}^{-1}$ )	$K_m$ ( $\mu\text{M}$ )	$k_{\text{cat}}$ ( $\text{s}^{-1}$ )	$k_{\text{cat}}/K_m$ ( $\text{M}^{-1} \text{s}^{-1}$ )
rVCPO	5.0	15.0	200	$1.3 \times 10^7$	1.15	23.0	$2.0 \times 10^4$	49.1	183	$3.7 \times 10^6$
	6.3	25.8	21.3	$8.3 \times 10^5$	10.2	7.3	$7.1 \times 10^2$	2.6	15.2	$5.8 \times 10^6$
S402A	5.0	15.3	81.7	$5.3 \times 10^6$	15.5	1.13	73.1	81.2	63.8	$7.9 \times 10^5$
	6.3	19.9	8.1	$4.1 \times 10^5$	174	1.42	8.1	1.3	6.4	$4.9 \times 10^6$
F397H	5.0	66.7	84.4	$1.3 \times 10^6$	16.4	6.5	$3.9 \times 10^2$	n.d.	n.d.	n.d.
	6.3	177	33.5	$1.9 \times 10^5$	474	5.7	12.0	n.d.	n.d.	n.d.

Parameters were determined by non-linear regression using EnzymeKinetics (Trinity Software). For experimental details for rVCPO and S402, see legends of Figs. 4–6. For the determination of F397H kinetic parameters, measurements were performed at a fixed  $\text{H}_2\text{O}_2$  concentration of 10 mM with at least six different halide concentrations. (n.d., not determined.)

#### 4.2. Haloperoxidase activity of F397H

The residue His478 in *A. nodosum* VBPO has been proposed as a likely candidate that confers preference for bromination rather than chlorination [5]. A VCPO variant F397H was designed to emulate the active site of VBPO in the VCPO and investigate the differential halogen oxidizing abilities of essentially conserved active sites. This mutation introduces an extra histidine (in place of phenylalanine) in the VCPO active site that corresponds to His478 in *A. nodosum* VBPO. Kinetic analysis of F397H presented here shows that the mutation caused a decrease in activity compared to the rVCPO. The relative brominating and chlorinating activities of F397H compared to rVCPO were 42% in bromination and 29% in chlorination, respectively at pH 5.0. Thus the effect of this mutation compared to other active site mutations (K353A, R360A, R490A and H496A) analysed by Hemrika et al. [7,18] is relatively mild. Although the only difference between VCPO and VBPO in the active site is the presence of this phenylalanine residue in VCPO where as in VBPOs it is a histidine, mutation of this residue did not convert rVCPO into an absolute bromoperoxidase. VBPO for example shows chlorination activity with high  $K_m$  value (344 mM, 0.49 U mg<sup>-1</sup> at pH 5) [25], but F397H still has a much higher affinity and rate of oxidation reaction ( $K_m$  for Cl<sup>-</sup> 16 mM, 5.8 U mg<sup>-1</sup> at pH 5.0). From these data the specificity constants  $k_{cat}/K_m$  for chloride are calculated to be 3.3 and 4.1 × 10<sup>2</sup> M<sup>-1</sup> s<sup>-1</sup> for VBPO and F397H, respectively (Table 1). Even though VBPO shows chlorinating activity, the specificity constant for chloride of F397H is a factor of 100 greater than that of VBPO. We conclude from our data that the difference in oxidative ability between VCPO and VBPO is not simply due to a single residue but apparently many factors are involved. We propose that the hydrogen bonding network in the active site and bound water molecules play an important role in the tuning of the reactivity of these enzymes.

The mutation had another significant effect on the activity during turnover. Although inhibition of VCPO and VBPO by excess halides has been reported previously [20], F397H was inhibited in somewhat different way. Both chloride and bromide bind relatively slowly to active site and once bound the enzyme is less active. Further there appears to be a competition between this halide binding site and peroxide. Lower concentrations of H<sub>2</sub>O<sub>2</sub> resulted in a much stronger inhibition by bromide.

As shown in Fig. 2 and Table 1, the F397H appears to be a better bromoperoxidase at high pH value ( $k_{cat} = 33.5$  s<sup>-1</sup> at pH 6.3) than rVCPO ( $k_{cat} = 21.3$  s<sup>-1</sup>). However to make such comparison, the specificity constant  $k_{cat}/K_m$  should also be taken into account. It is obvious that as shown in Table 1, that the mutant is

affected in catalytic activity. The  $k_{cat}/K_m$  decreased from 8.3 × 10<sup>5</sup> M<sup>-1</sup> s<sup>-1</sup> for rVCPO to 1.9 × 10<sup>5</sup> M<sup>-1</sup> s<sup>-1</sup> for the F397H mutant. A previous study by Hemrika et al. [7] showed that the mutants R360A and R490A revealed higher bromoperoxidase activity at high pH ( $k_{cat} = 333$  s and 239 s<sup>-1</sup> at pH 6.3, respectively) than rVCPO, although the specificity constants for both mutants were also lower than that of rVCPO because of the increase in  $K_m$ . In the terms of specificity constant, a mutant with the higher  $k_{cat}/K_m$  values than that of rVCPO has not been found yet. However, our results indicate that by mutagenesis it is possible to modulate the kinetic properties and modify the pH activity profile of these enzymes and that it should also be possible to shift the optimal pH of the enzyme activity.

#### Acknowledgements

This work was supported by the Council of Chemical Sciences of the Netherlands Organization for scientific research. The authors thank Dr. W. Hemrika for providing the *C. inaequalis* VCPO (pTNT 14) gene and Dr. R. Renirie for useful discussions.

#### References

- [1] E. de Boer, Y. van Kooyk, M.G.M. Tromp, H. Plat, R. Wever, *Biochim. Biophys. Acta* 869 (1986) 48.
- [2] J.W.P.M. van Schijndel, E.G.M. Vollenbroek, R. Wever, *Biochim. Biophys. Acta* 1161 (1993) 249.
- [3] A. Messerschmidt, R. Wever, *Proc. Natl. Acad. Sci. USA* 93 (1996) 392.
- [4] A. Messerschmidt, L. Prade, R. Wever, *Biol. Chem.* 378 (1997) 309.
- [5] M. Weyand, H.-J. Hecht, M. Kiess, M.-F. Liaud, H. Vilter, D. Schomburg, *J. Mol. Biol.* 293 (1999) 864.
- [6] M.N. Isupov, A.R. Dalby, A.A. Brindley, Y. Izumi, T. Tanabe, G.N. Murshudov, J.J. Littlechild, *Mol. Biol.* 299 (2000) 1035.
- [7] W. Hemrika, R. Renirie, S. Machedo-Ribeiro, A. Messerschmidt, R. Wever, *J. Biol. Chem.* 274 (1999) 23820.
- [8] W. Hemrika, R. Renirie, H.L. Dekker, P. Barnett, R. Wever, *Proc. Natl. Acad. Sci. USA* 94 (1997) 2145.
- [9] J. Stukey, G.M. Carman, *Protein Sci.* 6 (1997) 469.
- [10] A.F. Neuwald, *Protein Sci.* 6 (1997) 1764.
- [11] W. Plass, *Angew. Chem.* 38 (1999) 909.
- [12] Q.-X. Zhang, C.S. Pilquill, J. Dewald, L.B. Berthiaume, D.N. Brindley, *Biochem. J.* 345 (2000) 181.
- [13] K. Ishikawa, Y. Mihara, K. Gondoh, E.-I. Suzuki, Y. Asano, *EMBO J.* 19 (2000) 2412.
- [14] N. Tanaka, Z. Hasan, R.-J. Sanders, A. Hartog, R. Wever, *Org. Biomol. Chem.* 1 (2003) 2833.
- [15] N. Tanaka, V. Dumay, Q. Liao, A.J. Lange, R. Wever, *Eur. J. Biochem.* 269 (2002) 2162.
- [16] H. Dau, J. Dittmer, M. Epple, J. Hanss, E. Kiss, D. Rehder, C. Schulzke, H. Vilter, *FEBS Lett.* 457 (1999) 237.
- [17] J.N. Carter, K.E. Beatty, M.T. Simpson, A. Bulter, *J. Inorg. Biochem.* 91 (2002) 59.
- [18] R. Renirie, W. Hemrika, R. Wever, *J. Biol. Chem.* 275 (2000) 11650.



- [19] E. de Boer, H. Plat, M.G.M. Tromp, R. Wever, M.C.R. Franssen, H.C. van der Plas, E.M. Meijer, H.E. Schoemaker, *Biotechnol. Bioeng.* 30 (1987) 607.
- [20] J.W.P.M. van Schijndel, P. Barnett, J. Roelse, E.G.M. Vollenbroek, R. Wever, *Eur. J. Biochem.* 225 (1994) 151.
- [21] P. Barnett, W. Hemrika, H.L. Dekker, A.O. Muijsers, R. Renirie, R. Wever, *J. Biol. Chem.* 273 (1998) 23381.
- [22] T.S. Smith, V.L. Pecoraro, *Inorg. Chem.* 41 (2002) 6754.
- [23] D. Rehder, C. Schulzke, H. Dau, C. Meinke, J. Hanss, M. Epple, *J. Inorg. Biochem.* 80 (2000) 115.
- [24] J. Littlechild, E. Garcia-Rodriguez, *Coord. Chem. Rev.* 237 (2003) 65.
- [25] H.S. Soedjak, A. Butler, *Inorg. Chem.* 29 (1990) 5015.